

Expanded perlite: potential for removing antibiotics from water

Bruna Martins Vicentin¹ and Raquel Dalla Costa da Rocha¹

¹Chemistry Department, Universidade Tecnológica Federal do Paraná, Pato Branco 85503-390, Brazil

This work aims to study the potential of expanded perlite (EP) for amoxicillin (AMX) removal in aqueous solution. For this purpose, chemical, morphological, and textural characteristics of the EP were evaluated, in addition to AMX removal by the adsorption process. The kinetic, isothermal, and thermodynamic parameters were also assessed. The EP presented an isoelectric point of 6.5 and a surface with hydroxyl bands, which favour the adsorption process. Air bubbles were sealed and randomly connected with each other, increasing the surface area relative to the adsorption sites. These non-porous or macro-porous sites demonstrate efficiency in the mechanisms of mass transfer. AMX removal was determined to be a pseudo-second-order process since the adsorption velocity was proportional to the square of the available adsorption sites and indicates heterogeneity in the surface interactions between the adsorbed molecules. Also, the interactions were considered multilayer for low concentrations and monolayer for high concentrations (Sips isotherm). The adsorption process was endothermic and utilised a physical adsorption mechanism. Considering that no modification treatment was applied to the EP, and due to its neutral isoelectric point, macropores, amorphous and dipole induction force (physical adsorption) characteristics, favourable affinity between EP and AMX was observed.

INTRODUCTION

Perlite is a natural glassy volcanic rock (composition: $\cong 75\%$ of SiO_2 ; $\cong 15\%$ of Al_2O_3) (Ghassabzadeh et al., 2010; Cabuk et al., 2018; Corregidor et al., 2019), termed expanded perlite (EP) after being rapidly heated for 760–1 200°C and consequently expanded up to 20 times its original volume (Alkan and Dogan, 2002; Cabuk et al., 2018; De Oliveira et al., 2019). EP is employed in the construction industry (Papa et al., 2018; Leyton-Vergara et al., 2019; Top et al., 2020; Jiang et al., 2020), composite structure (Rodriguez et al., 2016; Ma et al., 2020; Rathore et al., 2020), agriculture and environmental sectors (Villaseñor et al., 2011; Torab-Mostaedi et al., 2011; Díez et al., 2020).

In the environmental sphere, the use of EP is efficient in removal of pollutants, such as heavy metals (Ghassabzadeh et al., 2010; Torab-Mostaedi et al., 2010; Torab-Mostaedi et al., 2011; Silber et al., 2012; Cabranes et al., 2018; Temel, 2018; Turp, 2018), petroleum hydrocarbons (Moussavi and Bagheri, 2012), among others (Heydartaemeh et al., 2014; Almeida et al., 2017; Da Silva Filho et al., 2018). EP has been studied for cetyltrimethylammonium bromide (Alkan et al., 2005), ciprofloxacin and isoniazid (Dube et al., 2018) drug removal. However, no previous studies have been reported on the use of EP for removal of amoxicillin in water.

Water contaminated by drug residues is problematic, since these residues affect human biological activities (Ali et al., 2016; Luo et al., 2018). Some water contaminants include analgesic, anti-inflammatory, and antibiotic drugs (Luo et al., 2018). Regarding antibiotics, the main concern is antibiotic resistance due to the reduction in treatment effectiveness for an ever-increasing range of infections caused by bacteria (WHO, 2014; Yu et al., 2020). Increasingly, scientists all over the world are on the alert for this serious public health problem.

The antibiotics contaminate the environment through pharmaceutical, domestic and hospital effluents that spread antibiotic at trace concentrations to drinking water, mainly as a result of the drainage and/or water furnishing system (surface water) (Ul Ain et al., 2018).

Amoxicillin ($\text{C}_{16}\text{H}_{19}\text{N}_3\text{O}_5\text{S}$) (AMX) is a broad-spectrum antibiotic derived from amino penicillin (β -lactam antibiotic). AMX is considered to be one of the most consumed antibiotics throughout the world, being prescribed to treat both human and animal infections (Githinji et al., 2011; Ul Ain et al., 2018).

The objective of this work was to study the potential of EP as an adsorbent in AMX removal and to evaluate the kinetic, isothermal, and thermodynamic parameters of the adsorption process.

METHODS

Antibiotic

AMX (98% in purity) was purchased from a manipulation pharmacy. Deionized water was employed to obtain the AMX stock solution ($50 \text{ mg}\cdot\text{L}^{-1}$).

Then the AMX solution was scanned by UV-VIS spectrophotometer (Thermo Scientific Evolution 60S) in the range 200–400 nm using deionized water as blank. The wavelength corresponding to maximum absorbance (λ_{max}) was found to be 223 nm.

CORRESPONDENCE

Raquel Dalla Costa da Rocha

EMAIL

raqueldcr@utfpr.edu.br

DATES

Received: 8 April 2020

Accepted: 30 September 2021

KEYWORDS

aluminosilicate
amoxicillin
adsorption
characteristics
mathematic modelling

COPYRIGHT

© The Author(s)
Published under a Creative
Commons Attribution 4.0
International Licence
(CC BY 4.0)

For the calibration curve, the stock solution was diluted to obtain a concentration ranging from 5 to 50 mg·L⁻¹. The relation between AMX concentration and absorbance presented linearity ($r^2 = 0.999$).

EP obtention and characterization

EP was received from Imerys – Perlite Paulínia Minerais Ltda, São Paulo, Brazil. The perlite was extracted from the Tucumán quarry in the province of Salta, Argentina. The expansion process was carried out in an oven at 900°C at the industrial unit of Banda del Río Salí, Argentina.

The isoelectric point of EP was determined by powder addition according to Mullet et al. (1997) with modifications. EP (50 mg) was added to 50 mL of NaCl solution (0.1 mol·L⁻¹), with the pH previously adjusted from 2 to 13 with HCl (0.1 mol·L⁻¹) and NaOH (0.1 mol·L⁻¹). After 24 h with constant agitation (180 r·min⁻¹) and temperature (25 ± 2°C) (Shaker Mod MAQL-200), the final pH was measured in triplicate.

Infrared (IR) spectral data were taken from a PerkinElmer FTIR Frontier spectrophotometer (400 – 4 000 cm⁻¹) at 2 cm⁻¹ resolution, using KBr pellets containing EP in the proportions of 99:1 mg. The X-ray diffractometry was determined using a diffractometer (XRD-Rigaku Mini flex 600). Finely ground samples of EP were dispersed onto the copper (Cu) sample holder and the data were collected from 3 to 90° with a step size of 0.05° and 1·s⁻¹ scanning speed.

In order to verify the morphology of the EP particles, a scanning electron microscope (SEM) (Hitachi TM3000) at 500× magnification was employed. The sample was previously exposed to thermal treatment at 300°C, for 24 h under vacuum to remove water, and the analyses were performed at 77 K using liquid nitrogen. Surface area measurement was performed by adsorption using nitrogen as adsorbate (Quantachrome NOVA 2000e).

EP potential for AMX removal

The experiments were carried out in a batch system. The triplicate assays were conducted in a bench orbital shaker at 28 ± 2°C and 150 r·min⁻¹. 1 g of EP was added to 100 mL AMX solution (pH 4.0; concentration: 50 mg·L⁻¹). At the end of each batch, the supernatant was set apart from solid material by filtration (Whatman – n° 1) and centrifugation (3 000 r·min⁻¹; 5 min) and submitted to spectrophotometric analysis at 223 nm to AMX determination.

Adsorption kinetics assays were conducted by AMX quantification from an aliquot of supernatant at each time frame.

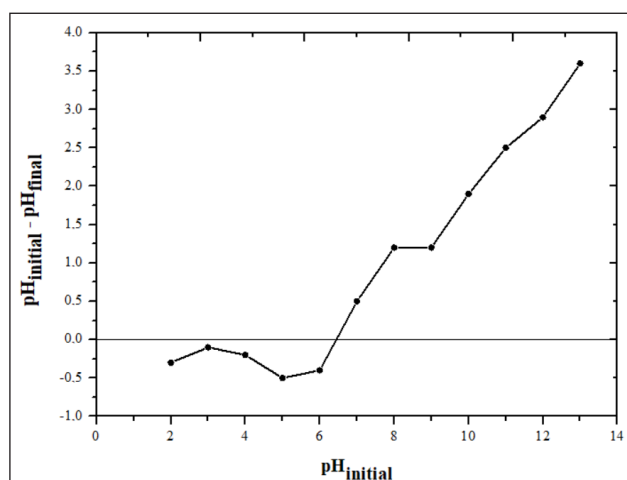


Figure 1. Isoelectric point of EP

The experimental data were fitted to pseudo-first-order (Yener et al., 2006) and pseudo-second-order (Blanchard et al., 1984) equations. The adsorption isotherm assay was performed for AMX concentrations of 5, 20, 35, and 50 mg·L⁻¹. Experimental data obtained for adsorption equilibrium studies were fitted to Langmuir (Langmuir, 1916), Freundlich (Freundlich, 1909) and Sips (Sips, 1948) isothermal models. The thermodynamic adsorption parameters were determined according to Gibbs free energy and Arrhenius equations from the adsorption equilibrium constant (Han et al., 2005), repeated at 25, 30, 35, and 40°C.

RESULTS AND DISCUSSION

EP characterization

The mineral EP used as adsorbent was previously characterized by textural, morphological, and functional group analyses.

As demonstrated in Fig. 1, the isoelectric point of EP was found to be 6.5, which indicates its capacity to be positively or negatively charged according to the medium pH.

Alkan et al. (2006) and Ghassabzadeh et al. (2010) found isoelectric points of 6.6 and 6.5, respectively. Alkan et al. (2005) confirmed the presence of silanol groups on EP, explaining that H⁺ ions can be replaced by Si-OH and Al-OH groups. This way, the acidic and alkaline properties of EP are attributed to the protonation and deprotonation of these groups. Although low and high pH values give rise to cationic and anionic complexes, respectively, the breaking up of O-H led to an increase in the negativity of the surface (Putra et al., 2009).

The main chemical groups identified in EP adsorbent for AMX removal are shown in Fig. 2.

The sample showed characteristic bands of the mineral. The broad band (3 626 cm⁻¹) between 3 450 and 3 600 cm⁻¹ was attributed to stretching vibrations of -OH groups on the surface of -Si-OH. The band at 1 641 cm⁻¹ was attributed to the bending mode of O-H from water molecules. The intense band at 1 061 cm⁻¹ was associated with the stretching vibrations of Si-O-Si structures. The bands at 783 and 454 cm⁻¹ were attributed to the stretching vibrations of Si-O and Al-O, respectively.

Similar results were reported for EP by Nasrollahzadeh et al. (2015), Cabuk et al. (2018), and De Oliveira et al. (2019). The interfaces of mineral particles are usually covered with hydroxyl groups formed by dissociative chemisorption of water. These groups act as effective adsorptive sites (Liu et al., 2017). This feature may be used as a guideline to obtain satisfactory adsorption results for EP in removing AMX.

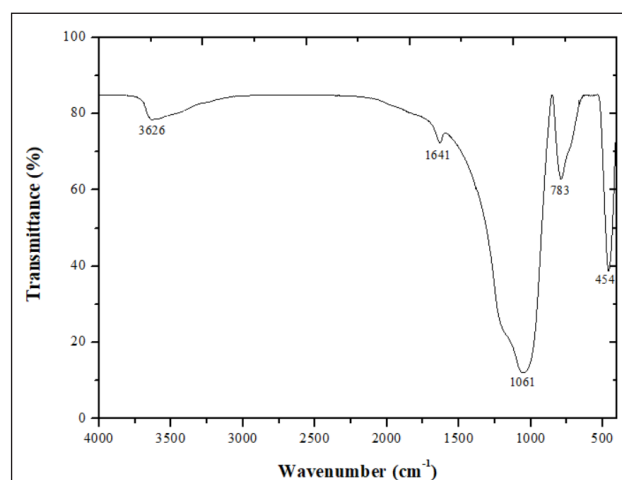


Figure 2. FTIR spectrum of the EP

The XRD pattern and SEM of the EP sample are presented in Fig. 3. The main peaks for EP were SiO₂ – 23.0° and 29.1° (Fig. 3a), classified in the ICSD database as characteristic of n° 00-029-005 (silicon oxide) and n° 01-085-0462 (quartz), respectively. This reflects the composition of the EP, of which silicon oxide constitutes 75%, with the rest made up of impurity phases, speculated to be aluminosilicate compounds in the structure (Tian et al., 2019). Also, through the XRD pattern results, EP was shown to be essentially amorphous, which is in accordance with literature (Celik et al., 2013; Almeida et al., 2017; De Oliveira et al., 2019).

The EP sample presented characteristic holes and thin walls (Tian et al., 2019; De Oliveira et al., 2019), an arrangement resulting from the perlite expansion process, in which the air bubbles are sealed and randomly connected to each other, increasing the relative surface area of the sites. This was confirmed by BET (Fig. 4, which presented a Type II isotherm curve (IUPAC, 1985), typical of material that has been submitted to a thermal expansion process (De Oliveira et al., 2019; Corregidor et al., 2019). The surface area of EP was found to be 1.6 m²·g⁻¹. Other investigators have reported surface areas of 1.8 m²·g⁻¹ (Ghassabzadeh et al., 2010), 1.7 m²·g⁻¹ (Nasrollahzadeh et al., 2015), and 2.0 m²·g⁻¹ (Corregidor et al., 2019).

Physicochemical aspects of AMX removal by EP

The amount of AMX adsorbed by EP increased rapidly in the first 7 min of the process, reaching equilibrium at around 20 min, with 2.700 mg·g⁻¹ of AMX adsorbed (51% removal). Maichin et al. (2013) found similar amounts of amoxicillin adsorption employing bentonite-magnetite (50%; 2.300 mg·g⁻¹), while Putra et al. (2009) obtained higher adsorption rates using bentonite (88%; 9.300 mg·g⁻¹) and activated carbon Norit ROW (95%; 10.000 mg·g⁻¹), and Zha et al. (2013) achieved 82% removal (21.600 mg·g⁻¹) when testing Na-montmorillonite.

Equilibrium for the process was considered to be reversible and fast, as a result of the molecules being physically attached to the adsorbent, weakening the intermolecular interactions. These intermolecular interactions originate from the attraction of induced permanent dipoles without changes in atomic

or molecular orbitals, known as Van der Waals adsorption (Farina et al., 1999).

The amount of AMX adsorbed per gram of EP at equilibrium was calculated by fitting kinetic models and was found to be very close to the experimental result – 2.701 mg·g⁻¹ for a pseudo-second-order equation (Table 1).

The pseudo-second-order model assumes that the adsorption speed is directly proportional to the square of available adsorption sites, suggesting that surface reactions control the process. The kinetic behaviour of EP corroborates the findings of other studies on the adsorption of silver, copper, mercury, caesium, lead and manganese (Ghassabzadeh et al., 2010; Cabranes et al., 2018; Temel, 2018; Turp, 2018).

The adsorption equilibrium assay was proposed to establish a relation between the amount of AMX removed and its residual concentration, providing information about the maximum adsorption capacity of the EP. From Langmuir, Freundlich, and Sips isothermal models, the amount of AMX and supernatant concentration were evaluated, and the isothermal parameters and correlation coefficients are given in Fig. 5 and Table 2.

The Sips model gave the best fit to the experimental data ($r^2 = 0.988$). The maximum AMX adsorption capacity of EP was 2.570 mg·g⁻¹. These results inferred that EP has heterogeneity in the adsorbent surface and the interactions between the adsorbed molecule were considered multilayer for low concentrations and monolayer for high concentrations (Foo and Hameed, 2010). The isotherm of the AMX adsorption process by EP was classified as Type V, in which the adsorbent-adsorbate interaction is weak, as obtained with certain porous adsorbents (IUPAC, 1985).

The increase in temperature described a non-spontaneous ($\Delta G > 0$) and endothermic process ($\Delta G = \text{decrease}$; $\Delta H = 27.045 \text{ kJ}\cdot\text{mol}^{-1}$). According to Castellan (1986), adsorption processes with energy below 42 kJ·mol⁻¹ may be considered as a physical adsorption. Thus, the results of this study indicate that the adsorption occurred by physisorption.

Due to significant changes in the FTIR results for EP after the adsorption process, our results confirm a physisorption process, as shown in Fig. 6.

Table 1. Kinetic parameters of AMX adsorption process in EP

Pseudo-first-order				Pseudo-second-order		
q _e experiment (mg·g ⁻¹)	q _e calculated (mg·g ⁻¹)	K ₁ (min ⁻¹)	R ²	q _e calculated (mg·g ⁻¹)	K ₂ (g·mg ⁻¹ ·min ⁻¹)	R ²
2.700	0.103	0.004	0.017	2.701	19.823	0.999

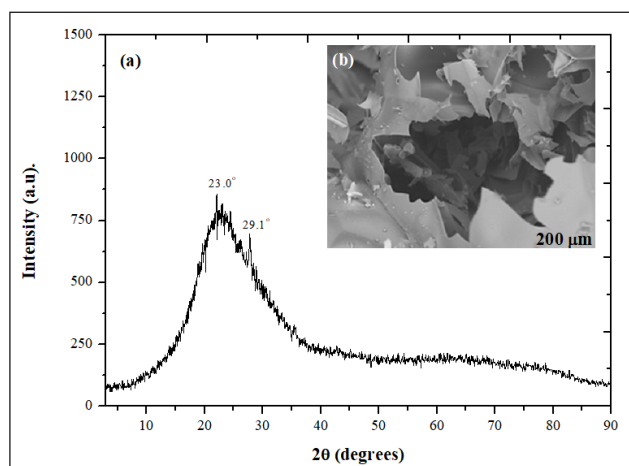


Figure 3. XRD pattern (a) of the EP. The inset (b) is an SEM image of the EP fracture

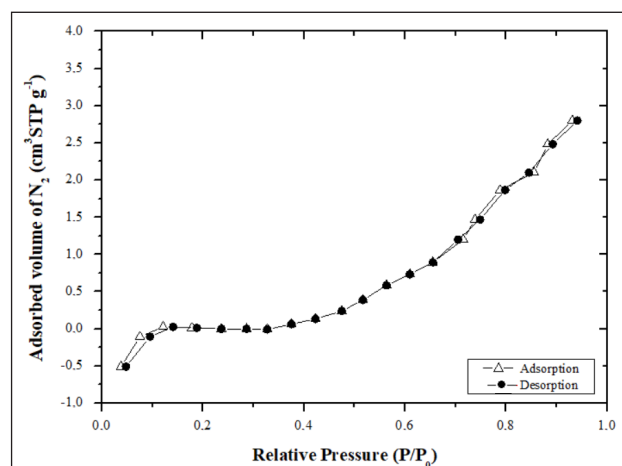
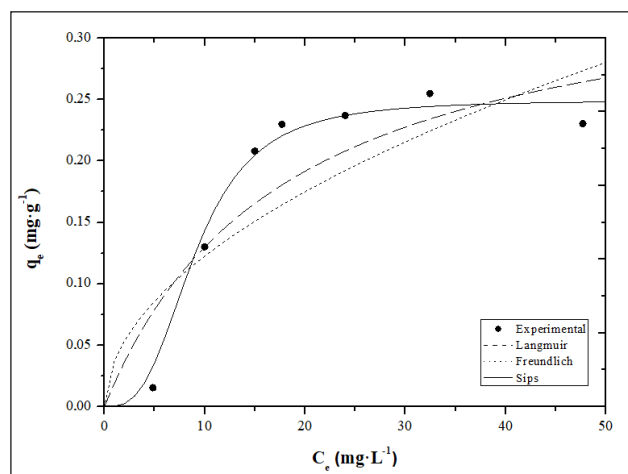
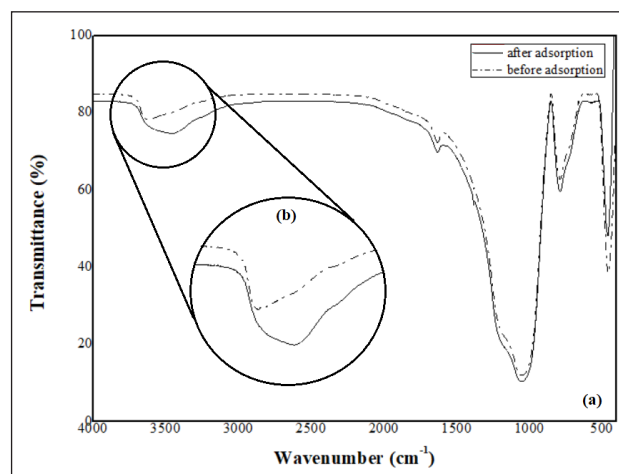


Figure 4. Adsorption/desorption N₂ isotherms

Table 2. Isotherm parameters of AMX adsorption process in EP

Parameter	Unit	Value	q_{\max} (mg·g ⁻¹)	N	r^2
Langmuir					
k_L	L·mg ⁻¹	0.066	1.364		0.882
Freundlich					
K_F	mg ^{1-(1/n)} ·g ⁻¹ ·L ^{1/n}	0.037		0.514	0.828
Sips					
k_S	(L·g ⁻¹) ^{1/n}	0.001	2.570	0.001	0.988

**Figure 5.** Langmuir, Freundlich, and Sips isotherms models for adsorption of AMX onto EP**Figure 6.** (a) FTIR of EP before (dotted line) and after (solid line) adsorption process; (b) magnification in the 300–3900 cm⁻¹ region

Since the process of AMX adsorption by EP was set as physisorption, there were no major variations in the functional groups of the adsorbent (Fig. 6a). The broadening and shifting in the region of 3000–3500 cm⁻¹ (Fig. 6b) was attributed to hydrogen bonds between –OH groups of EP and the hydrogen of hydroxyl and amino groups of AMX, which was also described by Ul Ain et al. (2018). Thus, for EP, there was no confirmation of modifications of functional groups, as is expected for physical adsorption, corroborating in part the results of the adsorption tests performed.

CONCLUSIONS

In seeking new materials for drug removal to reduce operating costs, it was necessary to study the degree of affinity between AMX and EP, in order to obtain an active and efficient adsorbent. Considering that considerable further research involving EP as adsorbent for drug removal is still required, the results obtained in this work indicate EP as a promising material for AMX removal by adsorption. The EP showed favourable physical-chemical characteristics, such as neutral isoelectric point, amorphous characteristics, and a physical adsorption process, which allows for it to be recycled for further use. Nonetheless, some other variables should be further explored to improve the ability of EP to remove AMX, such as chemical composition, mass quantity and particle size of EP, pH variation of the solution, desorption, and reuse.

ACKNOWLEDGEMENTS

This paper was financially supported by CAPES. The authors are grateful to UFPR-Curitiba and UTFPR Analysis Center.

REFERENCES

ALI I, AL-OTHMAN ZA and ALWARTHAN A (2016) Synthesis of composite iron nano adsorbent and removal of ibuprofen drug residue from water. *J. Mol. Liq.* **219** 858–864. <https://doi.org/10.1016/j.molliq.2016.04.031>

- ALKAN M, DEMIRBAŞ Ö, DOĞAN M and ARSLAN O (2006) Surface properties of bovine serum albumin – adsorbed oxides: Adsorption, adsorption kinetics and electrokinetic properties. *Micropor. Mesopor. Mater.* **96** (1-3) 331–340. <https://doi.org/10.1016/j.micromeso.2006.07.007>
- ALKAN M and DOĞAN M (2002) *Encyclopedia of Surface and Colloid Science*. Marcel Dekker, New York. 897 pp.
- ALKAN M, KARADAŞ M, DOĞAN M and DEMIRBAŞ Ö (2005) Adsorption of CTAB onto perlite samples from aqueous solutions. *J. Colloid Interface Sci.* **291** (2) 309–318. <https://doi.org/10.1016/j.jcis.2005.05.027>
- ALMEIDA JMF, OLIVEIRA ES, SILVA IN, DE SOUZA SPMC and FERNANDES NS (2017) Adsorption of erichrome black T from aqueous solution onto expanded perlite modified with orthophenanthroline. *Rev. Virtual Quim.* **9** (2) 502–513. <https://doi.org/10.21577/1984-6835.20170029>
- BLANCHARD G, MAUNAYE M and MARTIN G (1984) Removal of heavy metals from waters by means of natural zeolites. *Water Res.* **18** (12) 1501–1507. [https://doi.org/10.1016/0043-1354\(84\)90124-6](https://doi.org/10.1016/0043-1354(84)90124-6)
- CABRANES M, LEYVA AG and BABAY PA (2018) Removal of Cs⁺ from aqueous solutions by perlite. *Environ. Sci. Pollut. Res.* **22** 1982–21992. <https://doi.org/10.1007/s11356-018-2283-9>
- CABUK M, YESIL TA and YAVUZ M (2018) Colloidal and viscoelastic properties of expanded perlite dispersions. *J. Intell. Mater. Syst. Struct.* **29** (1) 32–40. <https://doi.org/10.1177/1045389X17698248>
- CASTELLAN GW (1986) *Fundamentos de fisico-química*. LTC, Rio de Janeiro. 552 pp.
- CELIK AG, KILIC AM and CAKAL GO (2013) Expanded perlite aggregate characterization for use as a lightweight construction raw material. *Physicochem. Probl. Miner. Process.* **49** (2) 689–700. <https://doi.org/10.5277/ppmp130227>
- CORREGIDOR PF, CUESTA PM, ACOSTA DE and DESTÉFANIS HA (2019) Composite ZSM-5/MCM-41 material obtained from a green resource and its enhanced catalytic performance in the reaction of vinyl acetate and isoamyl alcohol. *Catal. A-Gen.* **587** 117262. <https://doi.org/10.1016/j.apcata.2019.117262>
- DA SILVA FILHO SH, VINACHES P and PERGHER SB (2018) Zeolite synthesis in basic media using expanded perlite and its application in Rhodamine B adsorption. *Mater. Lett.* **227** 258–260. <https://doi.org/10.1016/j.matlet.2018.05.095>

- DE OLIVEIRA AG, JANDORNO JC, DA ROCHA EBD, DE SOUSA AMF and DA SILVA ALN (2019) Evaluation of expanded perlite behavior in PS/Perlite composites. *Appl. Clay Sci.* **181** 105223. <https://doi.org/10.1016/j.clay.2019.105223>
- DÍEZ AM, PAZOS M and SANROMÁN MA (2020) Bifunctional floating catalyst for enhancing the synergistic effect of LED-photolysis and electro-Fenton process. *Sep. Purif. Technol.* **230** 115880. <https://doi.org/10.1016/j.seppur.2019.115880>
- DUBE C, TANDLICH R and WILHELM B (2018) Adsorptive removal of ciprofloxacin and isoniazid from aqueous solution. *Nov. Biotechnol. et Chim.* **17** (1) 16–28. <https://doi.org/10.2478/nbec-2018-0002>
- FARINA C, SANTOS FC and TORT AC (1999) A simple way of understanding the nonadditivity of Van der Waals dispersion forces. *Am. J. Phys.* **67** (4) 344–349.
- FOO KY, HAMEED BH (2010) Insights into the modeling of adsorption isotherm systems. *Chem. Eng. J.* **156** (1) 2–10. <https://doi.org/10.1016/j.cej.2009.09.013>
- FREUNDLICH H (1909) The theory of adsorption. *Z. Phys. Chem.* **3** 212–220.
- GHAZZABZADEH H, MOHADESPOUR A, TORAB-MOSTAEDI M, ZAHERI P, GHANNADI M and TAHERI H (2010) Adsorption of Ag, Cu and Hg from aqueous solutions using expanded perlite. *J. Hazardous Mater.* **177** (1-3) 950–955. <https://doi.org/10.1016/j.jhazmat.2010.01.010>
- GITHINJI LJM, MUSEY MK and ANKUMAH RO (2011) Evaluation of the fate of ciprofloxacin and amoxicillin in domestic wastewater. *Water Air Soil Pollut.* **219** 191–201. <https://doi.org/10.1007/s11270-010-0697-1>
- HAN R, ZHANG J, ZOU W, SHI J and LIU H (2005) Equilibrium biosorption isotherm for lead ion on chaff. *J. Hazardous Mater.* **125** (1-3) 266–271. <https://doi.org/10.1016/j.jhazmat.2005.05.031>
- HEYDARTAEEMH M, DOULATI ARDEJANI F, BADII K, SEIFPANAHI SHABANI K and MOUSAVI S (2014) FeCl₂/FeCl₃ perlite nanoparticles as a novel magnetic material for adsorption of green malachite dye. *Arab. J. Sci. Eng.* **39** 3383–3392. <https://doi.org/10.1007/s13369-014-0978-x>
- IUPAC (1985) Reporting physisorption data for gas/solid systems with special reference to the determination of surface area and porosity. *Pure Appl. Chem.* **54** (11) 2201–2218.
- JIANG L, JIA G, JIANG C and LI Z (2020) Sugar-coated expanded perlite as a bacterial carrier for crack-healing concrete applications. *Constr. Build. Mater.* **232** 117222. <https://doi.org/10.1016/j.conbuildmat.2019.117222>
- LANGMUIR I (1916) The constitution and fundamental properties of solids and liquids. *J. Am. Chem. Soc.* **38** (11) 2221–2295. <https://doi.org/10.1021/ja02268a002>
- LEYTON-VERGARA M, PÉREZ-FARGALLO A, PULIDO-ARCAS J, CÁRDENAS-TRIVIÑO G and PIGGOT-NAVARRETE J (2019) Influence of granulometry on thermal and mechanical properties of cement mortars containing expanded perlite as a lightweight aggregate. *Materials (Basel)*. **12** (23) 4013. <https://doi.org/10.3390/ma12234013>
- LIU C, MA Q, HE H, HE G, MA J, LIU Y and WU Y (2017) Structure-activity relationship of surface hydroxyl groups during NO₂ adsorption and transformation on TiO₂ nanoparticles. *Environ. Sci. Nano.* **4** (12) 2388–2394. <https://doi.org/10.1039/c7en00920h>
- LUO Z, FAN, S, LIU J, LIU W, SHEN X, WU C, HUANG Y, HUANG G, HUANG H and ZHENG M (2018) A 3D stable metal-organic framework for highly efficient adsorption and removal of drug contaminants from water. *Polymers.* **10** (2) 209. <https://doi.org/10.3390/polym10020209>
- MA B, JIN Z, SU Y, LU W, QI H and HU P (2020) Utilization of hemihydrate phosphogypsum for the preparation of porous sound absorbing material. *Constr. Build. Mater.* **234** 117346. <https://doi.org/10.1016/j.conbuildmat.2019.117346>
- MAICHIN F, FREITAS LC and ORTIZ N (2013) The use of converter slag (magnetite) and bentonite clay for amoxicillin adsorption from polluted water. *Orbital: Eletron. J. Chem.* **5** (3) 1–5. <https://doi.org/10.17807/orbital.v5i3.494>
- MOUSAVI G and BAGHERI A (2012) Removal of petroleum hydrocarbons from contaminated groundwater by the combined technique of adsorption onto perlite followed by the O₃/H₂O₂ process. *Environ. Technol.* **33** (16) 1905–1912. <https://doi.org/10.1080/09593330.2011.650223>
- MULLET M, FIEVET P, REGGIANI JC and PAGETTI J (1997) Surface electrochemical properties of mixed oxide ceramic membranes “Zeta-potential and surface charge density. *J. Membr. Sci.* **123** (2) 255–265. [https://doi.org/10.1016/S0376-7388\(96\)00220-7](https://doi.org/10.1016/S0376-7388(96)00220-7)
- NASROLLAHZADEH M, SAJADI SM, ROSTAMI-VARTOONI A, BAGHERZADEH M and SAFARI R (2015) Immobilization of copper nanoparticles on perlite: Green synthesis, characterization and catalytic activity on aqueous reduction of 4-nitrophenol. *J. Mol. Catal. A-Chem.* **400** 22–30. <https://doi.org/10.1016/j.molcata.2015.01.032>
- PAPA E, MEDRI V, MURRI A, LAGHI L, DE ALOYSIO G, BANDINI S and LANDI E (2018) Characterization of alkali bonded expanded perlite. *Constr. Build. Mater.* **191** 1139–1147. <https://doi.org/10.1016/j.conbuildmat.2018.10.086>
- PUTRA EK, PRANOWO R, SUNARSO J, INDRASWATI N and ISMADJI S (2009) Performance of activated carbon and bentonite for adsorption of amoxicillin from wastewater: mechanisms, isotherms and kinetics. *Water Res.* **43** (9) 2419–2430. <https://doi.org/10.1016/j.watres.2009.02.039>
- RATHORE PKS, SHUKLA SK and GUPTA NK (2020) Synthesis and characterization of the paraffin/expanded perlite loaded with graphene nanoparticle as a thermal energy storage material in buildings. *J. Sol. Energy Eng.* **142** (4) 041006. <https://doi.org/10.1115/1.4046087>
- RODRIGUEZ J, SORIA F, GERONAZZO H and DESTEFANIS H (2016) Modification and characterization of natural aluminosilicates, expanded perlite, and its application to immobilise α-amylase from *A. oryzae*. *J. Mol. Catal. B Enzym.* **133** (1) S259–S270. <https://doi.org/10.1016/j.molcatb.2017.01.012>
- SILBER A, BAR-YOSEF B, SURYANO S and LEVKOVITCH I (2012) Zinc adsorption by perlite: Effects of pH, ionic strength, temperature, and pre-use as growth substrate. *Geoderma.* **170** 159–167. <https://doi.org/10.1016/j.geoderma.2011.11.028>
- SIPS R (1948) On the structure of a catalyst surface. *J. Chem. Phys.* **16** 490–495. <https://doi.org/10.1063/1.1746922>
- TEMEL FA (2018) Endüstriyel sızıntı suyundan Pb (ii) giderimi için geliştirilmiş perlit Kullanımı: Kinetik çalışmalar. *Türk Tarım Gıda Bilim ve Teknol. Derg.* **6** (3) 360–364. <https://doi.org/10.24925/turjaf.v6i3.360-364.1748>
- TIAN Y, TANG Y, LI S, LV H, LIU P and JING Q (2019) Voigt-based swelling water model for super water absorbency of expanded perlite and sodium polyacrylate resin composite materials. *E-Polymers.* **19** (1) 365–368. <https://doi.org/10.1515/epoly-2019-0038>
- TOP S, VAPUR H, ALTINER M, KAYA D and EKICIBİL A (2020) Properties of fly ash-based lightweight geopolymer concrete prepared using pumice and expanded perlite as aggregates. *J. Mol. Struct.* **1202** 127236. <https://doi.org/10.1016/j.molstruc.2019.127236>
- TORAB-MOSTAEDI M, GHAEMI A, GHAZZABZADEH H and GHANNADI-MARAGHEH M (2011) Removal of strontium and barium from aqueous solutions by adsorption onto expanded perlite. *Can. J. Chem. Eng.* **89** (5) 1247–1254. <https://doi.org/10.1002/cjce.20486>
- TORAB-MOSTAEDI M, GHAZZABZADEH H, GHANNADI-MARAGHEH M, AHMADI SJ and TAHERI H (2010) Removal of cadmium and nickel from aqueous solution using expanded perlite. *Braz. J. Chem. Eng.* **27** (2) 299–308. <https://doi.org/10.1590/S0104-66322010000200008>
- TURP S (2018) Mn²⁺ and Cu²⁺ adsorption with a natural adsorbent: Expanded perlite. *Appl. Ecol. Env. Res.* **16** (4) 5047–5057. https://doi.org/10.15666/aeer/1604_50475057
- UL AIN N, ANIS I, AHMED F, SHAH MR, PARVEEN S, FAIZI S and AHMED S (2018) Colorimetric detection of amoxicillin based on quercetageitin coated silver nanoparticles. *Sensor Actuat B-Chem.* **265** 617–624. <https://doi.org/10.1016/j.snb.2018.03.079>
- VILLASEÑOR J, RODRÍGUEZ L and FERNÁNDEZ J (2011) Composting domestic sewage sludge with natural zeolites in a rotary drum reactor. *Bioresour. Technol.* **102** (2) 1447–1454. <https://doi.org/10.1016/j.biortech.2010.09.085>
- WHO (2014) *Antimicrobial Resistance: Global Report on Surveillance.* World Health Organization, Geneva. 256 pp.
- YENER J, KOPAC T, DOGU G and DOGU T (2006) Adsorption of basic yellow 28 from aqueous solutions with clinoptilolite and amberlite. *J. Colloid Interface Sci.* **294** (2) 255–264. <https://doi.org/10.1016/j.jcis.2005.07.040>

YU K, LI P, CHEN Y, ZHANG B, HUANG Y, HUANG FY and HE Y (2020) Antibiotic resistome associated with microbial communities in an integrated wastewater reclamation system. *Water Res.* **173** 115541. <https://doi.org/10.1016/j.watres.2020.115541>

ZHA SX, ZHOU Y, JIN X and CHEN Z (2013) The removal of amoxicillin from wastewater using organobentonite. *J. Environ. Manage.* **129** 569–576. <https://doi.org/10.1016/j.jenvman.2013.08.032>
